48th International Conference on Environmental Systems
8–12 July 2018, Albuquerque, New Mexico
ICES-2018-192

Integrated Oxygen Flow Meter/Heat Exchanger for Portable Life Support Systems

Michael G. Izenson,[1] Amelia T. Servi[2] Scott D. Phillips[3], and Sheldon X. Stokes[4]
Creare LLC, Hanover, NH 03755

and

Colin Campbell[5]
NASA Lyndon B. Johnson Space Center, Houston, TX, 77058

Space suits for future exploration missions will have multi-mission goals with new and challenging requirements for the portable life support system (PLSS). In particular, the space suit ventilation loop requires cooling and flow measurement components that must meet specifications that go well beyond the capabilities of the components used for the existing Extravehicular Mobility Unit. The flow meter must have high measurement accuracy over a wide flow range, compatibility with pure oxygen, low pressure losses, and very compact size. The heat exchanger that cools the ventilation loop must be built from materials that are compatible with the liquid cooling loop, and it must provide efficient gas cooling in a small package across conditions ranging from normal suit pressure to elevated pressure. This paper describes the development of a novel device that combines the flow measurement and cooling functions in a single, compact flow meter/heat exchanger (FMHX). We have developed design methods that enable us to assess trade-offs, optimize performance, and specify the design of an FMHX that meets the requirements and constraints for operation in future PLSSs. We used empirical design correlations combined with computational fluid dynamics analysis to design the FMHX design. Data from tests of a proof-of-concept FMHX validate the design methods and show that the device meets all design requirements. We used the results from these tests to refine the design parameters and predict performance of an optimized, prototype FMHX.

Nomenclature

CFD	=	computational fluid dynamics
EMU	=	Extravehicular Mobility Unit
EVA	=	extravehicular activity
FMHX	=	flow meter/heat exchanger
PLSS	=	portable life support system

I. Introduction

Portable Life Support Systems (PLSSs) for future exploration space suits are being developed to meet new and very challenging requirements. These systems must be designed for long-duration exploration missions to destinations very far from Earth. They will be used for planetary and lunar exploration activities in ways that require much greater mobility than provided by the existing ISS Extravehicular Mobility Unit (EMU). As a result, new system components and new capabilities are required that meet goals for high performance, compact size, and light weight. Development of new, miniaturized PLSS technology is therefore a critical goal for NASA's program to

[1] Principal Engineer, Creare LLC
[2] Engineer, Creare LLC
[3] Engineer, Creare LLC
[4] Engineer, Creare LLC
[5] xEMU PLSS Lead, Crew and Thermal Systems Division, NASA Johnson Space Center

develop an exploration PLSS. Multifunctional components that can provide more than one capability in a single, compact package would be uniquely valuable.

This paper presents results of a project to prove the feasibility of a multifunction flow meter/heat exchanger (FMHX) for the ventilation loop in next-generation PLSSs. The FMHX is designed to provide an accurate measurement of oxygen flow across a wide range of operating conditions while also cooling the ventilation gas to a comfortable temperature before it flows back into the space suit pressure garment. We proved the feasibility of making an FMHX that meets NASA's requirements through thermal, fluid, and mechanical design; fabrication and assembly of a proof-of-concept FMHX; and measuring the performance of the proof-of-concept FMHX in laboratory tests that simulated operation in a space suit ventilation loop. The proof-of-concept FMHX met all thermal and flow requirements with significant margin. Based on these results, we then produced a design for a prototype, compact FMHX designed to integrate with NASA's PLSS demonstration systems. The flight-like unit fits within the required volume specifications with a predicted mass of 1.18 kg.

FMHX design requirements for flow rate, pressure drop, heat transfer, and measurement accuracy were provided by NASA. To meet these requirements, we designed and built a miniature shell-and-microtube heat exchanger in which the ventilation gas flows through the tube side. The microtube array also serves as a highly linear pressure drop element for measuring the gas flow rate. We also designed and built a flow test facility that enabled us to accurately measure the performance of the FMHX across a range of gas pressures and flow rates that simulate conditions specified for operation in future PLSSs. We used a miniature, oxygen-compatible electronic sensor to measure the pressure drop across the microtube array.

II. FMHX Function and Requirements

A. Function

The FMHX is designed for use in the PLSS's oxygen ventilation loop, where it will measure the ventilation flow rate and cool the ventilation gas before it re-enters the pressure garment. The FMHX is located in between the CO_2 absorber beds and the gas inlet coupling with the pressure garment. Ventilation gas flows through the absorber beds prior to entering the FMHX, where CO_2 and nearly all the moisture are removed. Because the dew point of the gas leaving the absorber beds is very low, no water will condense in the FMHX. Cooling water for the FMHX is supplied by the circulating pump in the thermal control loop. The FMHX is located immediately downstream of the pumps.

B. Requirements

The FMHX is designed to meet measurement, flow, and heat transfer requirements based on the PLSS design for the advanced EMU. When operating in the PLSS, the FMHX coolant will be ultrapure water dosed with biocide, and the ventilation gas will be propellant-grade oxygen, along with a small percentage of other gases such as nitrogen evolved during the crew pre-breathe, CO_2/H_2O loading, etc.

The nominal accuracy requirement of the flow meter is ±1% of the full range of gas flow, or 1.7 L/min. out of 170 L/min.

Other PLSS performance requirements flow down to the FMHX as limitations on pressure drops and temperature differences between the gas and liquid under specified flow conditions. Table 1 lists the pressure drop and flow requirements for both the water and gas sides of the heat exchanger.

Table 1. Flow and pressure drop requirements.

Side of Heat Exchanger	Water		Gas	
Temperature	10.0°C	[50°F]	15.6°C	[60°F]
Pressure	Not specified	Not specified	29.7 kPa	[4.3 psia]
Flow Rate for ΔP Spec	90.7 kg/hr	[200 lb_m/hr]	170 act. L/min.	[6 act. ft^3/min.]
Maximum Pressure Drop	5.5 kPa	[0.80 psid]	170 ± 20 Pa	[0.68 ± 0.07 in. H_2O]
Flow Rate Range	77.0 to 99.8 kg/hr	[170 to 220 lb_m/hr]	Not specified	Not specified

The heat exchanger must cool the ventilation gas before it flows back into the pressure garment. To define the required cooling, the heat exchanger performance requirements specify the maximum temperature difference between the gas outlet and the cooling water inlet under three key operational conditions, listed in Table 2. Design point 3 is based on use of the EVA suit for hyperbaric treatment. This high pressure operating point turns out to be the most challenging heat transfer requirement despite the relatively large temperature difference (7.2°C) allowed

between the gas outlet and water inlet. The amount of heat transfer for design point 3 is much larger than for design points 1 and 2 since the mass flow rate of gas is much higher when the loop runs at high pressure. Table 2 lists the pressures, temperatures, and flow rates for each operating condition as well as the maximum gas-to-liquid temperature difference.

Table 2. Heat exchanger design points and performance requirements.

Design Point	Suit Pressure	Ventilation Flow Rate	Maximum Oxygen Inlet Temperature	Nominal Thermal Loop Inlet Temperature	Minimum Thermal Loop Flow Rate	Max ΔT: Ventilation Loop Outlet Minus Thermal Loop Inlet
1	29.6 kPa [4.3 psia]	127 lpm [4.5 acfm]	32°C [90°F]	13°C [55°F]	77 kg/h [170 pph]	2.8°C [5°F]
2	29.6 kPa [4.3 psia]	170 lpm [6.0 acfm]	32°C [90°F]	13°C [55°F]	77 kg/h [170 pph]	4.4°C [8°F]
3	157 kPa [22.7 psia]	170 lpm [6.0 acfm]	32°C [90°F]	13°C [55°F]	77 kg/h [170 pph]	7.2°C [13°F]

In addition to limits on pressure losses and gas outlet temperature, the FMHX must also satisfy requirements for proof, burst, and collapse pressures; high measurement accuracy; size; and materials.

III. Flow Meter/Heat Exchanger Design

A. Design Concept

The FMHX comprises a miniature shell-and-tube heat exchanger in which the ventilation gas flows through the tube side and cooling water flows through the shell side. The small-diameter tubes provide a very large heat transfer area in a small volume, allowing the FMHX to meet heat transfer requirements with minimum volume. Laminar flow through the microtubes has a very favorable heat transfer/pressure drop characteristic, so that a compact core built with the microtubes can meet requirements for low pressure loss. The tubes also have a very long aspect ratio, and as a result have highly linear flow vs. Δp characteristics. Measuring the pressure drop due to gas flow through the heat exchanger can therefore provide an accurate measurement of the gas flow rate.

Figure 1 shows a cross-sectional view of the FMHX with the key elements visible, including a honeycomb flow straightener, the microtube array, and the pressure taps on either side of the microtube array. Figure 2 shows the flow paths of the ventilation gas and the cooling water through the FMHX. The gas and water flow in a counter/cross-flow arrangement to maximize heat transfer. Three baffles force the water to cross the microtube array four times between the inlet and outlet, which ensures good cooling of all the tubes and increases heat transfer between the water and the gas. The overall design shown in Figure 1 and Figure 2 (with a cylindrical shell and external tie rods for assembly) corresponds to the proof-of-concept unit that was built and tested to prove feasibility. A flight unit would be much more compact (Section VII).

A short length of honeycomb is placed in the gas flow directly upstream of the heat exchanger core. The purpose of the honeycomb is to prevent large secondary flows that are generated at the oxygen inlet port from persisting at the inlet to the heat exchanger core. If secondary flows were to generate large gas velocities perpendicular to the tube axes, then the upstream pressure measurement would be confounded by the associated dynamic head.

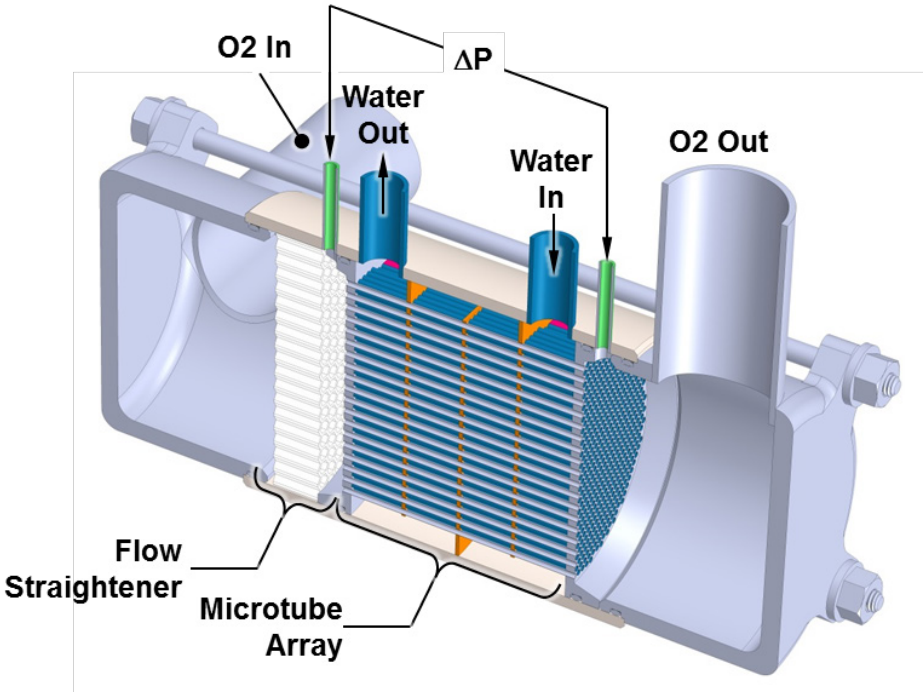

Figure 1. Overall design of the FMHX.

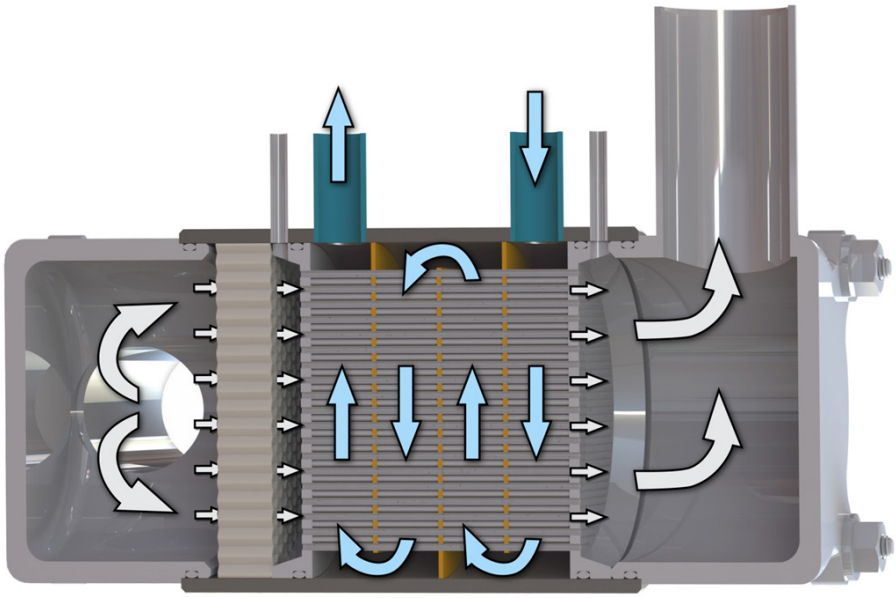

Figure 2. Ventilation gas and cooling water flow paths.

The pressure drop across the microtube array will be measured with a miniature flow sensor coupled to the pressure taps indicated in Figure 1. These taps represent the ends of two capillary tubes, which provide a high-resistance flow path between the microtube array's gas inlet and gas exit faces. The capillary tubes will lead into and out of a miniature flow sensor, and the measured flow rate will be proportional to the differential pressure across the microtube array. This differential pressure, in turn, can be used to calculate the volumetric flow rate in the ventilation loop. We have identified several compact, COTS flow sensors that are oxygen safe and potentially suitable for use in the FMHX. These sensors typically use a thermal measurement technique that provides an output signal that is highly linear with respect to flow rate, making them a good choice for the large range of flow rates to be measured. As described later in this paper, we validated the measurement accuracy and vibration insensitivity of one of these sensors in bench tests of the FMHX.

B. Heat Exchanger Design Methods

Because of the complex geometries of the heat exchanger and Reynolds numbers that lie within the transition region, correlations were more useful for predicting performance than analytical models. Our main source for pressure loss estimations for the gas and water loops was the *Handbook of Hydraulic Resistance* by I. E. Idelchik.[1] We used *Compact Heat Exchangers* by W. M. Kays and A. L. London[2] for additional pressure loss and heat exchanger effectiveness estimations, and we used *A Heat Transfer Textbook* by J. H. Lienhard V and J. H. Lienhard V[3] to estimate heat transfer coefficients.

Computational Fluid Dynamics. We used computational fluid dynamics (CFD) to assess the flow distribution on the gas side of the heat exchanger. Because the FMHX must meet very tight volume constraints, there is not enough space available for large manifolds or plena. The pressure drop across the microtube array must be large enough to distribute the gas flow uniformly through all the microtubes. If the flow is not uniform, then the heat transfer correlations will not be accurate and performance may fall short of requirements.

To model the gas flow through the heat exchanger, we approximated the microtube core as a porous element with anisotropic permeability. We specified a permeability in the direction of the tube axes to match the flow resistance of the high aspect-ratio tubes (corrected for the actual tube flow area). The permeability perpendicular to the tube axes was set to zero. This approximation allows modeling of the phenomena that determine the flow distribution through the core without an unreasonably large computational grid. We used the same approach to model the flow straightener. The CFD calculations were made using ANSYS™ Fluent® release 16.2.

Figure 3 shows calculated pathlines through the entire heat exchanger assembly, and Figure 4 shows the pressure distribution at the inlet to the microtube array. Figure 3 shows that the honeycomb does a good job conditioning the flow just upstream of the microtube array while occupying a relatively small volume. The pathlines in Figure 3 are color-scaled by velocity magnitude, and they show that the velocity through the heat exchanger core is highly uniform. The gas pressure distribution at the tube inlet (Figure 4) also shows very little variation, consistent with highly uniform flow through the microtube array.

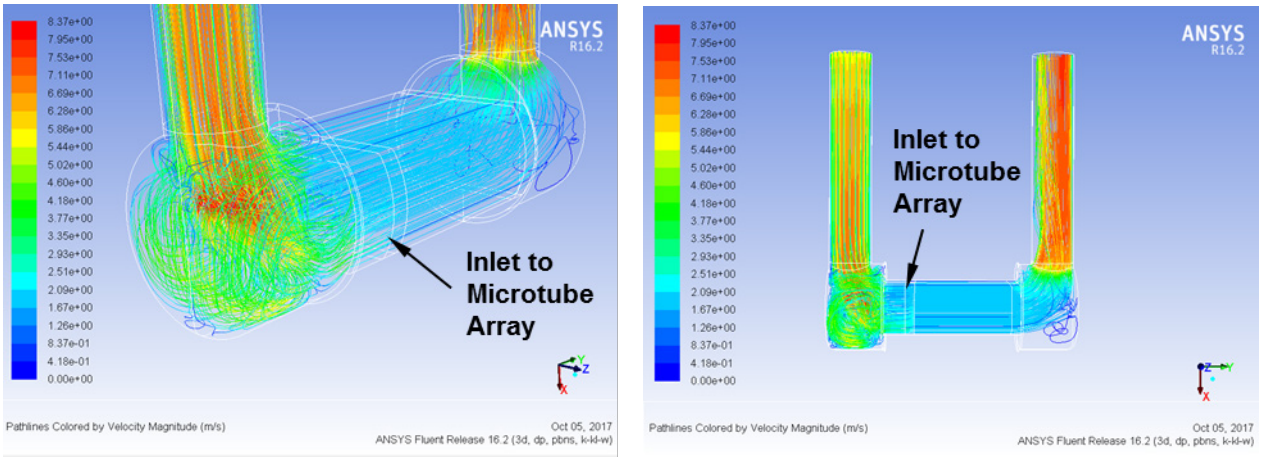

(a) Pathlines colored by velocity magnitude (b) Side view of pathlines

Figure 3. CFD calculations predict highly uniform flow through the microtube array. The static pressure distribution at the inlet face of the microtube array is shown in Figure 4.

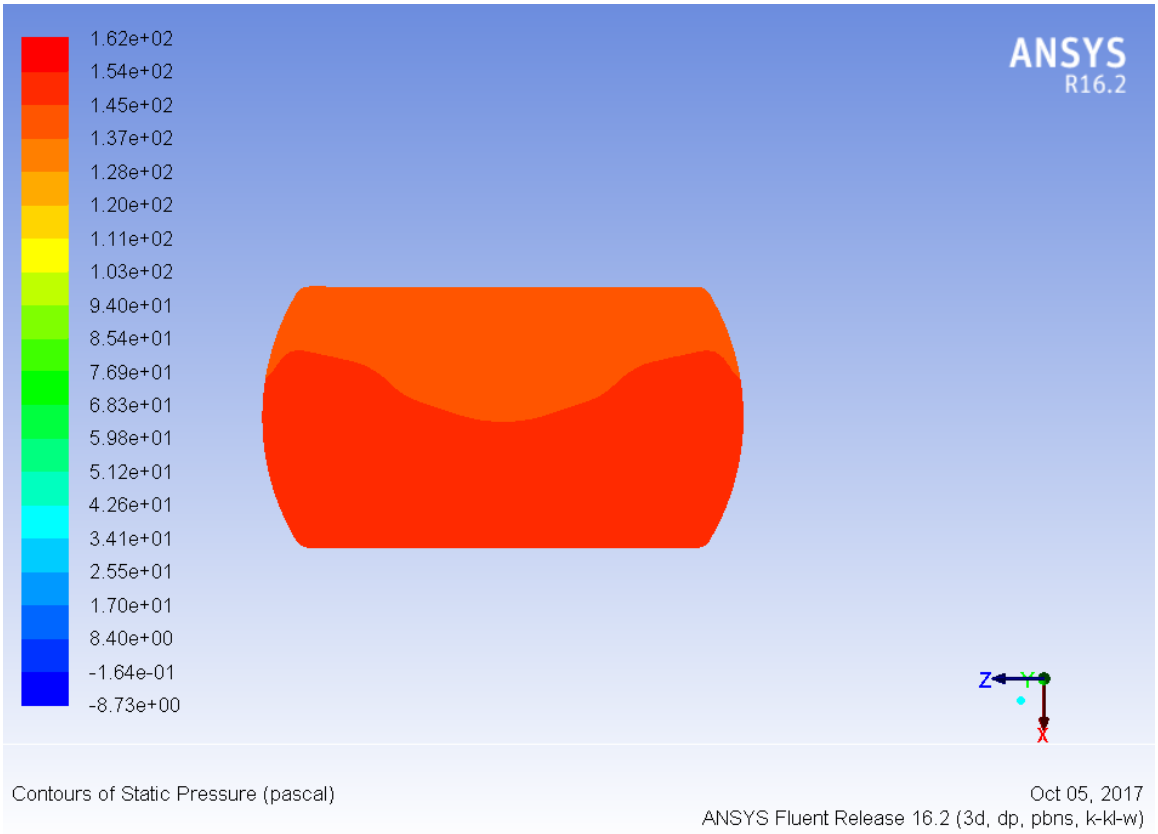

Figure 4. CFD predicts very little variation in static pressure across the inlet face of the microtube array.

IV. Fabrication of a Proof-of-Concept FMHX

The proof-of-concept FMHX comprises a heat exchanger core that is built into a housing/flow manifold assembly (Figure 5). The heat exchanger core is an array of small-diameter microtubes that are welded into tube sheets at both ends. The heat exchanger core was designed by Creare and assembled by Mezzo Technologies (Baton Rouge, LA). We specified stainless steel for the proof-of-concept unit because these tubes were readily available off the shelf. Inconel® tubes will be needed for future prototypes for compatibility with other materials in the space suit thermal control loop. Inconel tubes are available with longer lead times and can also be made into microtube arrays. The manifold assembly was fabricated at Creare.

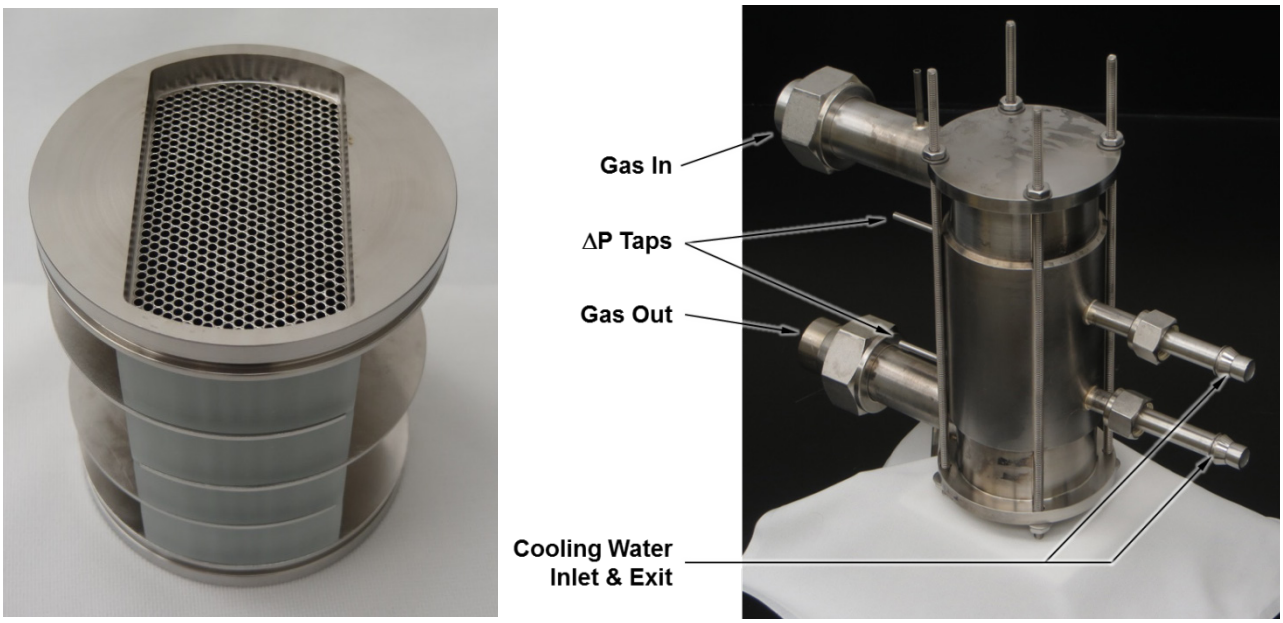

Figure 5. Microtube core (left) and assembled FMHX (right).

V. Measuring Performance of the FMHX

We assembled a test facility to measure performance of the FMHX under conditions that simulate operation in a space suit life support system. The facility was designed to confirm that the FMHX meets the requirements for operation in the advanced EMU PLSS. The facility was configurable in two modes: (1) low-pressure testing to simulate normal PLSS operation, and (2) high-pressure testing to simulate operation during hyperbaric treatment.

Table 3 lists the instruments we used to measure the FMHX performance. All instrumentation (along with all tubing and valves) is oxygen compatible, although all testing to date has used pure nitrogen on the gas side.

Table 3. Instrumentation.

Instrument	Designation in Schematics	Type	Accuracy
Analog pressure gauge	P1, P4	McMaster-Carr 32255K6 0-100 psi	2 psi graduation marks
Analog pressure gauge	P3	McMaster-Carr 32255K6 0 to 30 psi	1 psi graduation marks
Pressure transducer	P2	Omega PX 605 30V15GI-X6B	+/-0.06 psi
Differential pressure transducers	ΔP1, ΔP2	Sensirion SDP611-500 Pa	+/-3% reading
Flow meter (in parallel with the Sensirion)	ΔP1, ΔP2	Posifa PMF2050V	+/-0.25 std cm^3/min.
Differential pressure transducer	ΔP3	Omega PX2300-5DI	+/- 0.0125 psi
T-Type thermocouples	T1-T5	Omega TMQSS-062U-6	+/-1 °C
Gas flow meter	FM1	Alicat MS-250SLPM-D/5M	+/-0.4% reading + 0.2% full scale
Water flow meter	FM2	Omega FLR101	+/- 0.05 L/min.

A. Testing at Low Pressure

Figure 6 illustrates the test facility configured for measuring performance at low pressure, and Figure 7 shows a photograph. The gas enters the system through a pressure regulator attached to a pressurized nitrogen or oxygen bottle. The gas then passes through a high-accuracy flow meter (FM1) and then through a gas conditioning heat exchanger to bring it to the test temperature. A needle valve then throttles the flow, bringing the pressure of the gas down to the test pressure. The pressure and temperature of the gas (T1, P2) are measured prior to entering FMHX,

and temperature is measured again at the FMHX exit (T2). The gas then enters the vacuum port of the ejector and is entrained with shop air and vented through the ejector outlet. The flow rate and pressure of the gas is controlled by adjusting the needle valve, the shop air pressure into the ejector (P4), and the inlet pressure (P1). An accumulator between the FMHX and the ejector smooths out high-frequency pressure variations caused by the ejector. Pressure ports on either side of the microtube array and on the FMHX inlet and outlet allow us to measure the pressure difference across the microtube array (ΔP1) and across the full FMHX (ΔP2). ΔP1 is part of the FMHX itself. ΔP2 is part of the test facility used to determine if the FMHX meets the pressure loss specification.

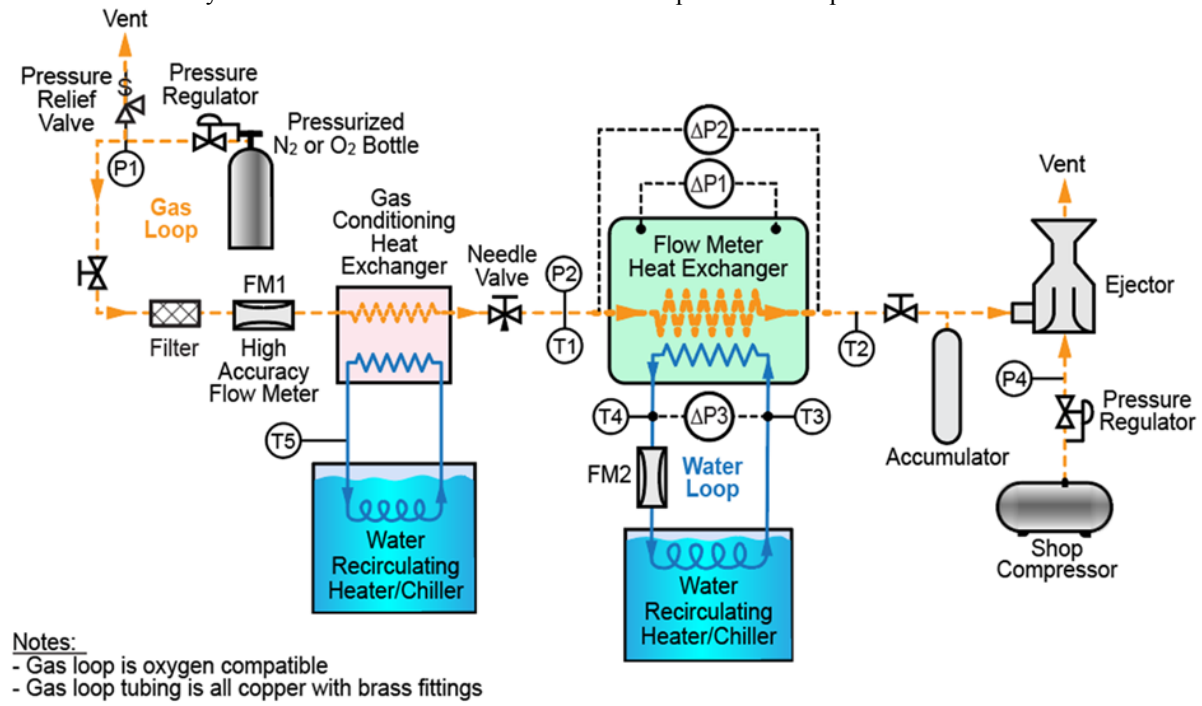

Figure 6. Test setup to measure FMHX performance during low-pressure operation.

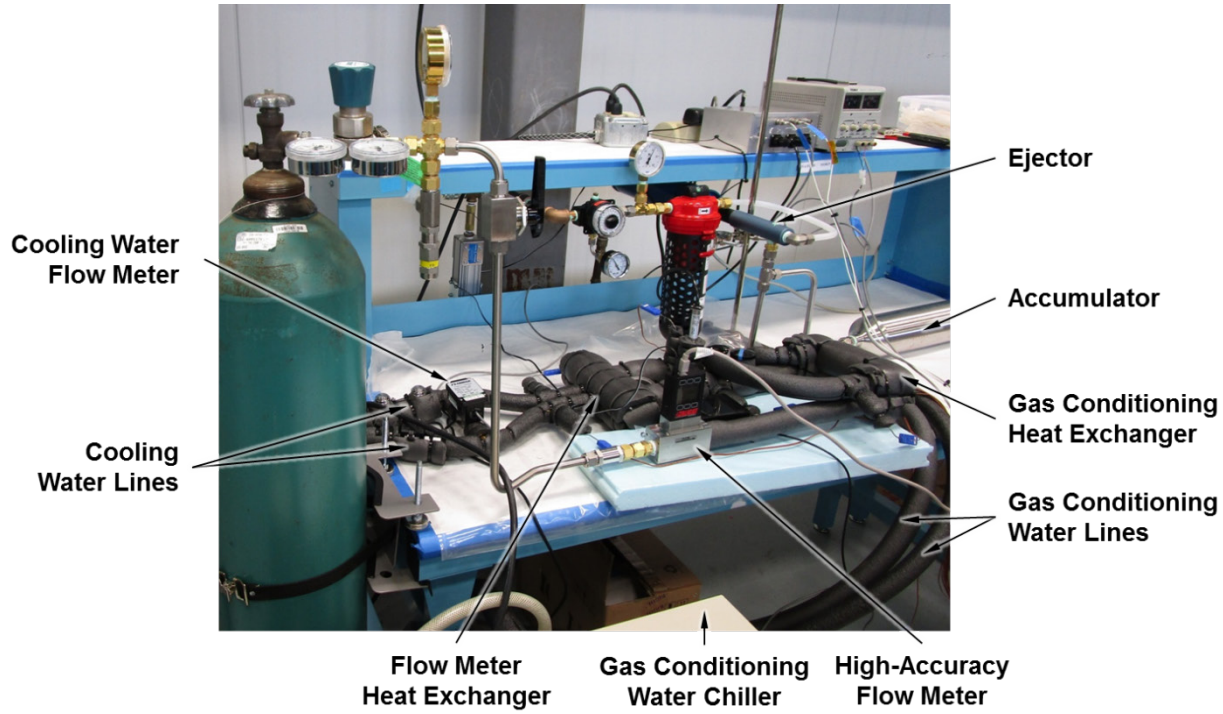

Figure 7. Photograph of test facility.

On the water side of the system, a recirculating heater/chiller supplies DI water to the water loop at a controlled temperature. The water passes through the FMHX and then through a flow meter (FM2). Temperature is measured before and after the FMHX (T3 and T4). The pressure drop across the FMHX is measured with a differential pressure transducer (ΔP3). A ball valve is used to control the water flow rate.

B. Testing at High Pressure

Figure 8 shows the test setup for measuring performance at high pressure. As with the low-pressure configuration, gas enters the system through a pressure regulator and passes through the high-accuracy flow meter, gas-conditioning heat exchanger, and FMHX. Temperature and pressure are measured at the same locations as the low-pressure configuration. Unlike the low-pressure configuration, the needle valve to control pressure is located downstream of the FMHX. After flowing past the needle valve, the gas vents to atmosphere. The flow rate and pressure of the gas is controlled by adjusting the inlet pressure (P1) and the needle valve. The water side of the system is unchanged from the low-pressure configuration.

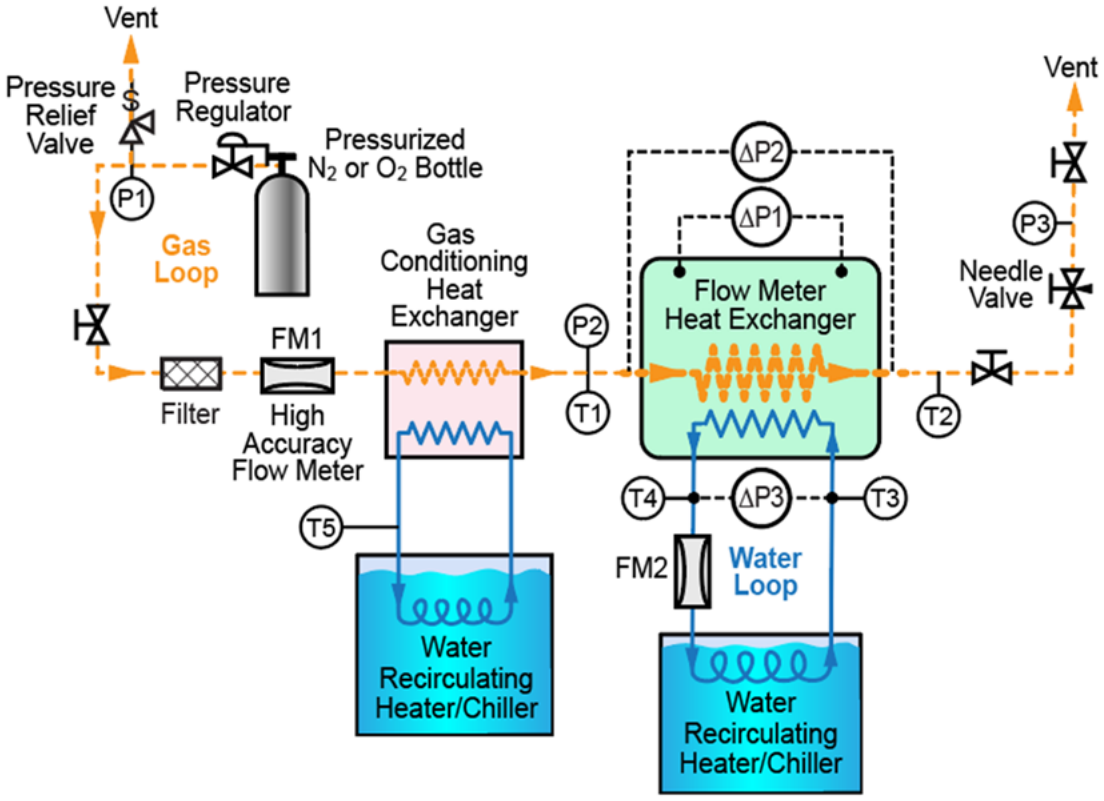

Figure 8. Test setup to measure FMHX performance during high-pressure operation.

V. Heat Transfer and Pressure Drop Performance

A. Gas-Side Pressure Loss

Figure 9 plots results of our pressure measurements at normal suit pressure (29.6 kPa or 4.3 psia). Also shown is the maximum specified pressure drop (for O_2 and scaled to N_2) and the predictions from our design model. The pressure drop across the entire FMHX meets the design requirement with good margin (about 30%). The flow vs. ΔP characteristics also agrees well with our design models for the microtube array. The pressure drop across the entire flow meter is about 20% less than predicted. This is not surprising, due to the complex nature of the flow in the components upstream and downstream from the microtube array and the conservatism of our design models.

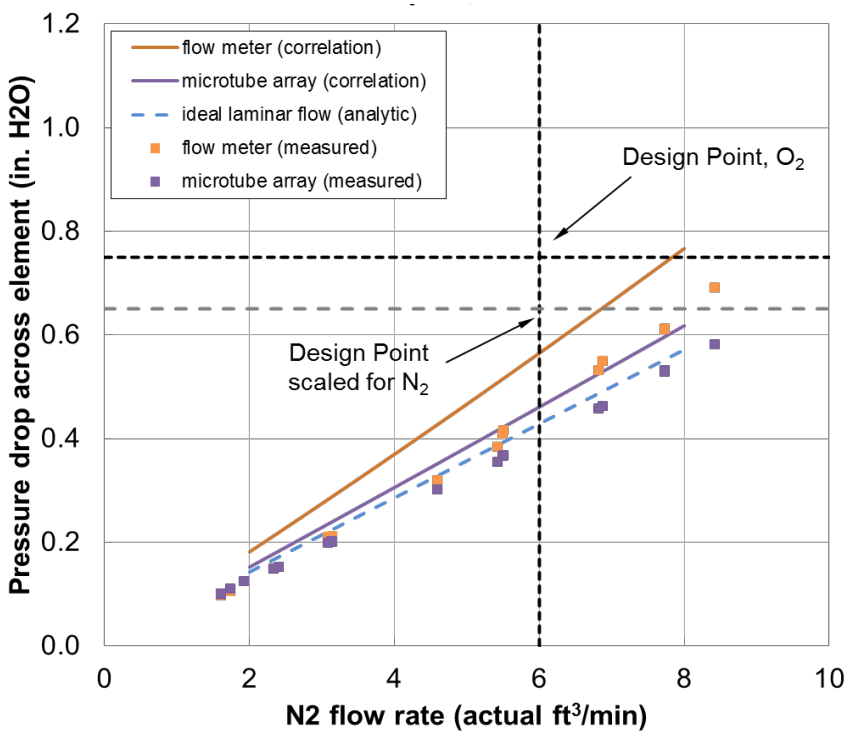

Figure 9. Pressure drop across flow meter and microtube array. "Flow meter" refers to the entire device (ΔP2 in Figure 8) and is significant relative to overall pressure drop requirements. "Microtube array" refers only to the pressure drop across the microtube array (ΔP1 in Figure 8), which will be used to deduce the gas flow rate (N_2 flow, 29.6 kPa/4.3 psia, 15.6°C). Note that 10 ft^3/min. = 4.7 L/s and 1.0 in. H_2O = 248 Pa.

Figure 10 shows the same data taken at a loop pressure 156 kPa (22.7 psia). The FMHX requirements do not specify a maximum pressure drop for high-pressure operation; however, the data show that the unit still meets the requirement for low-pressure operation when operating at high pressure. Also in this case, the flow vs. ΔP characteristics agree well with our design models for both the microtube array and the FMHX as a whole.

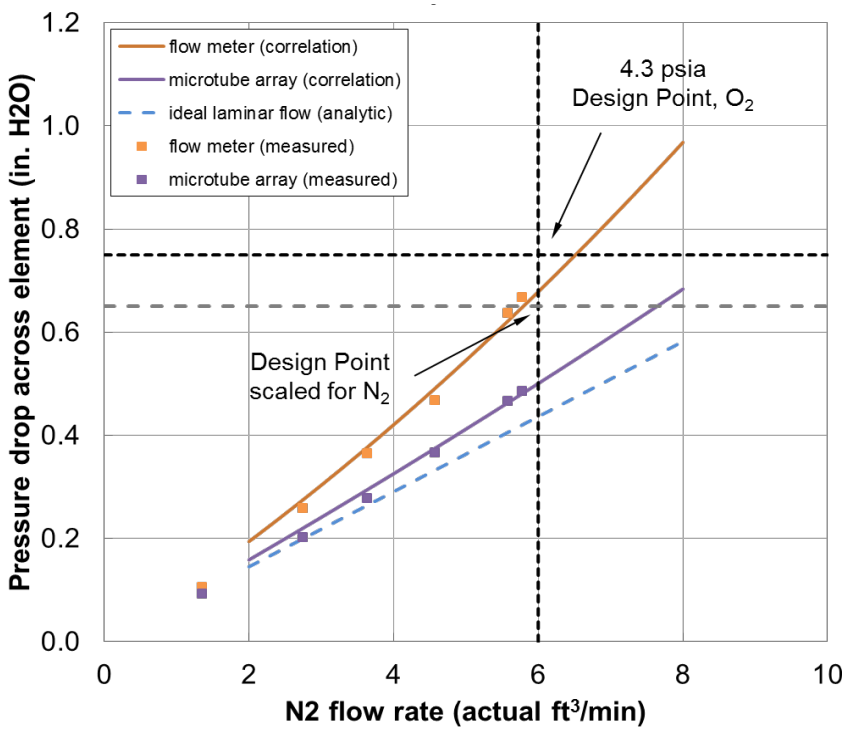

Figure 10. Pressure drop across flow meter and microtube array "Flow meter" refers to the entire device (ΔP2 in Figure 8) and is significant relative to overall pressure drop requirements. "Microtube array" refers only to the pressure drop across the microtube array (ΔP1 in Figure 8), which will be used to deduce the gas flow rate (N_2 flow, 156 kPa/22.7 psia, 24°C). Note that 10 ft^3/min. = 4.7 L/s and 1.0 in. H_2O = 248 Pa.

B. Water-Side Pressure Loss

The water-side pressure loss meets the design requirement and agrees well with our design models. Figure 11 plots the water-side pressure drop as a function of flow rate, and also shows the predicted flow vs. ΔP characteristics and the design requirement. At the nominal flow rate of 0.025 kg/s (200 lb_m/hr), the measured pressure drop of about 3.7 kPa is about 30% lower than the maximum specified value of 5.5 kPa. The measured results are also in reasonably good agreement with the predictions of the design model.

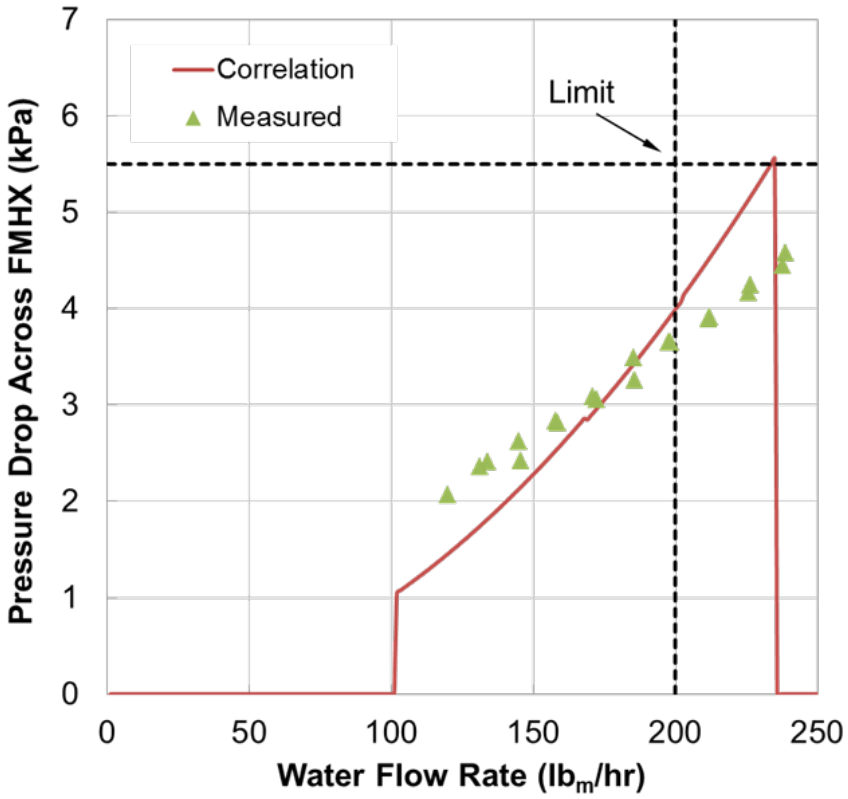

Figure 11. Pressure drop due to water flow through the microtube array (note 250 lb_m/hr = 31.5 g/s).

C. Gas Cooling

The FMHX exceeds the gas-cooling requirements. Figure 12 shows the difference between gas exit temperature and water inlet temperature as a function of gas flow rate measured at normal loop operating pressure. The gas inlet temperature T1 (32°C according to the specification) varied between 30°C and 33°C; data are shown from two test series where the inlet temperature was slightly high (31°C to 33°C) and slightly low (30°C to 32°C). In both cases, the temperature difference between the gas outlet and water inlet was about 1°C or less—well under the requirement (3.0°C to 4.5°C, depending on the gas flow rate). The data suggest that the gas temperature becomes slightly cooler (roughly 0.25°C) with increasing flow rates. This is unexpected behavior that we have not had time to fully explore. It is possible that higher flow rates result in increased gas mixing at the heat exchanger outlet. This effect could change the temperature measured by the thermocouple without necessarily meaning that the average gas exit temperature is falling at higher flow rates.

Figure 13 shows the gas exit temperature measured at high loop pressure. The gas leaving the FMHX is 5°C or more cooler than the specification, and in good agreement with the predictions of our design model.

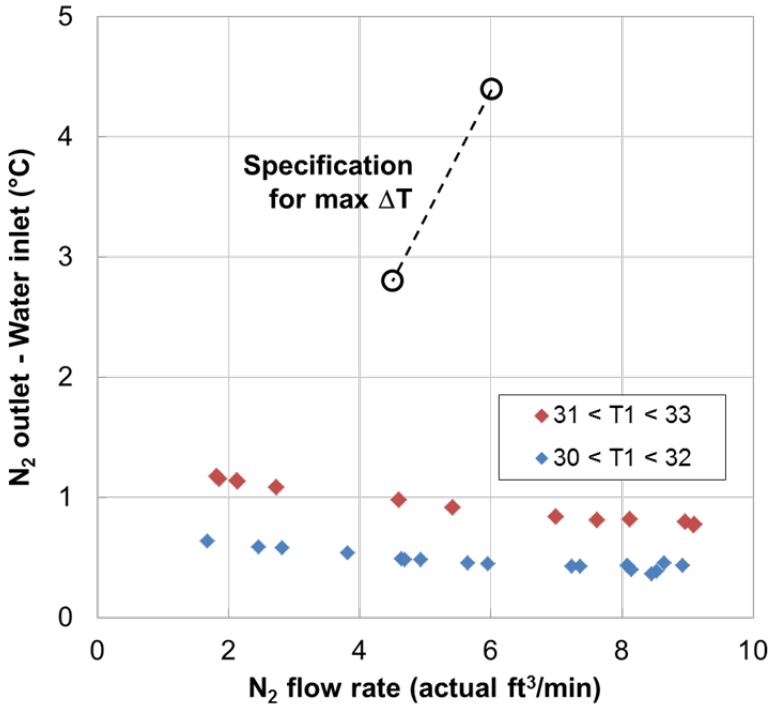

Figure 12. Cooling performance at low pressure (29.6 kPa/4.3 psia, 32°C N_2 inlet, 13°C water inlet). Note that 10 ft^3/min. = 4.7 L/s.

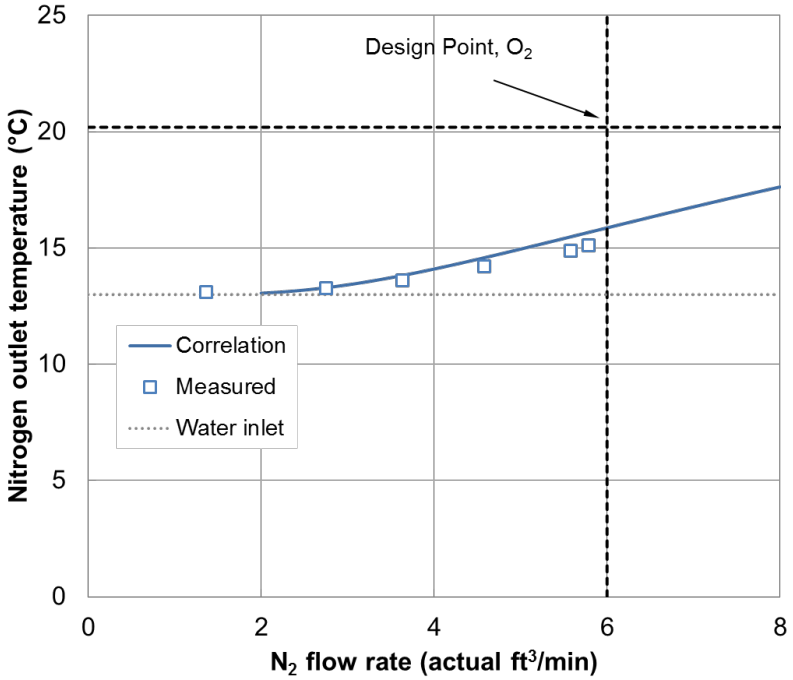

Figure 13. Cooling performance at high pressure (156 kPa/22.7 psia, 32°C N_2 inlet, 13°C water inlet). Note that 8 ft^3/min. = 3.8 L/s.

Table 4 summarizes the pressure drop and heat transfer requirements for the FMHX, along with the results from Phase I testing. The proof-of-concept unit met all the requirements with significant margin. Pressure losses were less than the specified maximum by about 30%, and the maximum gas exit temperature was lower than the maximum specified by at least 2°C.

Table 4. The proof-of-concept FMHX met all performance requirements.

		O_2 Loop Only	H_2O Loop Only	Heat Exchange Between Loops		
	Measurement	**Spec 1: Max ΔP across meter**	**Spec 2: Max ΔP across meter**	**Spec 3: Max $T_{O2,in}$ low pressure, low flow**	**Spec 4: Max $T_{O2,in}$, low pressure, high flow**	**Spec 5: Max $T_{O2,in}$, high pressure, high flow**
Conditions	O_2 flow rate (act ft^3/min.)	6		4.5	6	6
	O_2 abs pressure (psia)	4.3		4.3	4.3	22.7
	O_2 inlet temp (°C)	15.6		32	32	32
	Water flow rate (lb_m/hr)		200	170	170	170
	Water abs press (psia)		14.7	14.7	14.7	14.7
	Water inlet temp (°C)		10	13	13	13
Required Performance	O_2 ΔP (in. H_2O)	0.68±0.07				
	Max O_2 outlet T (°C)			15.8	17.4	20.2
	Max water ΔP (kPa)		5.5			
Status		Demonstrated (29% margin)	Demonstrated (34% margin)	Demonstrated (~2°C margin)	Demonstrated (~3°C margin)	Demonstrated (~5°C margin)

D. Flow Rate Measurement

To use the FMHX as a flow meter, it must be possible to accurately and repeatably relate the gas flow rate to the pressure drop measured across the microtube array. For best accuracy across the entire flow range, the pressure drop should be a highly linear function of the flow rate and it must be possible to measure the pressure drop accurately with a compact sensor that is suitable for use in space flight.

The proof-of-concept unit has demonstrated a highly linear pressure drop vs. flow characteristic. Figure 14 shows data from nitrogen flow tests at a pressure of 4.3 psia and a temperature of 15.6°C. The pressure drop was measured across the pressure taps immediately upstream and downstream of the microtube array for flow rates in the range of 2.0 to 8.5 actual ft^3/min. The linear fit to the data has an R^2 value of 0.9993, showing that the heat exchanger has good potential to serve as a linear pressure drop element for flow measurement. The actual pressure drop is roughly 11% lower than the pressure drop predicted using standard relations for laminar flow through circular tubes. The difference is probably due to a combination of several factors, including uncertainties in the gas temperature (which affects the viscosity) and variation in tube ID about the mean (which will tend to reduce overall pressure losses). For use as a high-accuracy flow meter, each microtube array will probably need to be calibrated for flow vs. pressure drop across the expected range of operating conditions.

We have also identified small commercial sensors that may be suitable for measuring the differential pressure in the FMHX. These types of sensors have been developed for medical oxygen service and should be easily adaptable for space flight. We measured the accuracy of these sensors against a calibrated differential pressure sensor and also showed that they were unaffected by vibration conditions that are typical of manned space flight. Figure 15 shows results of the vibration tests, demonstrating that the sensor is highly accurate and insensitive to prototypical vibration levels. Figure 15a plots data separately for calibration runs before, during, and after the vibration testing. The sensor response is highly linear and does not change due to vibration. Figure 15b plots all the data as a single set along with a linear fit. The R^2 value of 0.9993 shows that the calibration data can be predicted using a linear fit with extremely high accuracy, regardless of the sensor's vibration history. Additional testing—particularly shock testing and rigorous spacecraft oxygen compatibility testing—will be needed before adopting any particular sensor for this application.

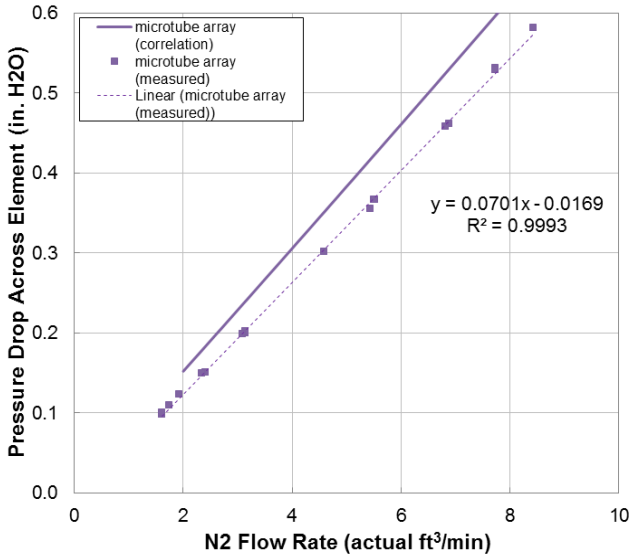

Figure 14. The pressure drop measured across the microtube array is highly linear with flow rate (test conditions: 4.3 psia, 15.6°C). Note that 10 ft^3/min. = 4.7 L/s and 1.0 in. H_2O = 248 Pa.

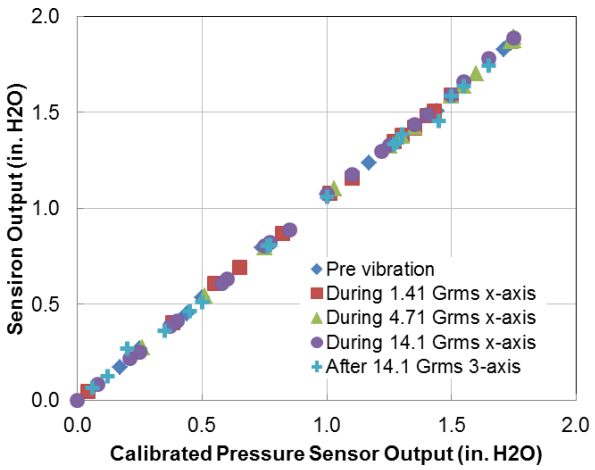

(a) Calibration before, during, and after vibration testing up to 14.1 Grms

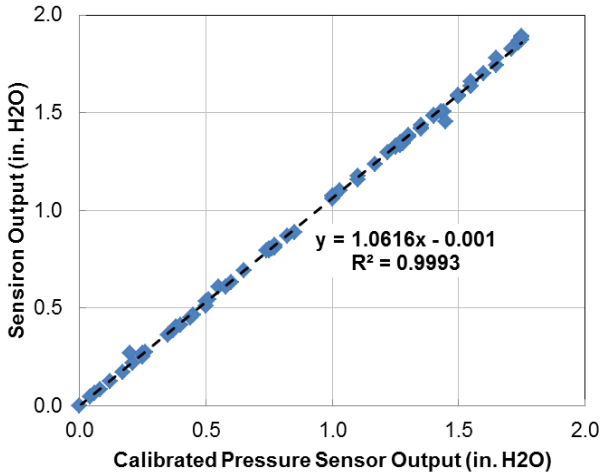

(b) Consolidated data from vibration test series and linear fit

Figure 15. The Sensirion transducer is highly linear and insensitive to vibration. Note 1 in. H_2O = 248 Pa.

VI. Validation of Design Models

Our design methods have been validated by comparison with performance data as well as comparison with CFD results. The methods are currently accurate enough to design the FMHX to meet pressure drop and heat transfer requirements. Use of the heat exchanger pressure drop to estimate gas flow rates will probably require each microtube core to be calibrated individually.

The gas-side pressure drop at high pressure (Figure 10) is predicted very well for both the microtube array and the heat exchanger as a whole. At lower pressure (Figure 9), the agreement is within 10% for the microtube array and within 20% for the entire heat exchanger. This level of agreement is satisfactory for design of the FMHX. To use the pressure drop as an accurate measure of gas flow rate, the flow vs. pressure drop characteristics for each microtube array should be calibrated individually to provide data for the flow rate calculation.

Water-side pressure drop (Figure 11) agrees reasonable well with our current design models, which are close enough to ensure that the performance meets specifications.

Predictions of the gas outlet temperature under the design-limiting conditions (Figure 13) are in close agreement with our design models. The CFD calculations for flow with heat transfer through the microtubes agree very closely with the isothermal calculations based on the analytic prediction for laminar, fully developed flow through a circular tube. The overall design to ensure uniform flow through and across the microtubes is validated by CFD results (Figure 3, Figure 4) and by very efficient heat transfer (Figure 12).

VII. Flight-Like Design

We have produced a design for a flight-like FMHX that shows the potential for future units to meet all performance requirements while also fitting into a compact package that will integrate well with a compact PLSS. Key features of the flight-like prototype are:

- The microtube array is fabricated from Inconel 625 instead of stainless steel for compatibility with titanium components in the thermal control loop. This change in material will not have a noticeable effect on the heat exchanger performance. Although the thermal conductivity of Inconel (~9.5 W/m-K) is less than that of stainless steel (~9.5 W/m-K), the thermal resistance due to heat conduction across the tube wall is two to three orders of magnitude smaller than the thermal resistance due to convection on the gas side.
- The microtube array contains the same number of tubes we used in the Phase I proof-of-concept unit.
- The flight-like unit is packaged in a rectangular housing for better form factor.
- The housing can be made from Inconel 625 (a heavier option), or the housing (and various other components) can be made from Ultem 1000 polyetherimide, which is a lightweight, oxygen-compatible plastic that can be machined with precise features.
- The flight-like unit has an integrated electronics enclosure for the differential pressure sensor.

The mass of the FMHX is predicted to be 1.18 kg (2.60 lb_m) if all components are made from Inconel. If Ultem 1000 is used for the housing, then the mass drops to 759 g (1.67 lb_m), and if Ultem 1000 is used for as many components as possible (inlet and outlet elbows, flow baffles, etc.), then the mass could be reduced to 385 g (0.85 lb_m). Figure 16 shows an overall and exploded view of the FMXH.

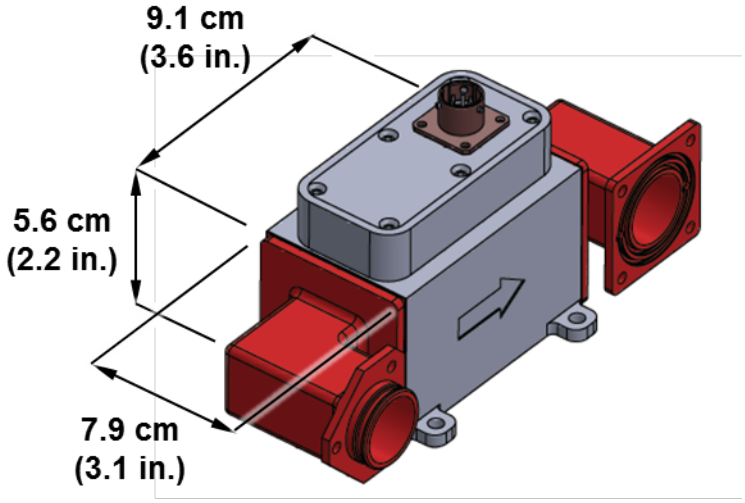

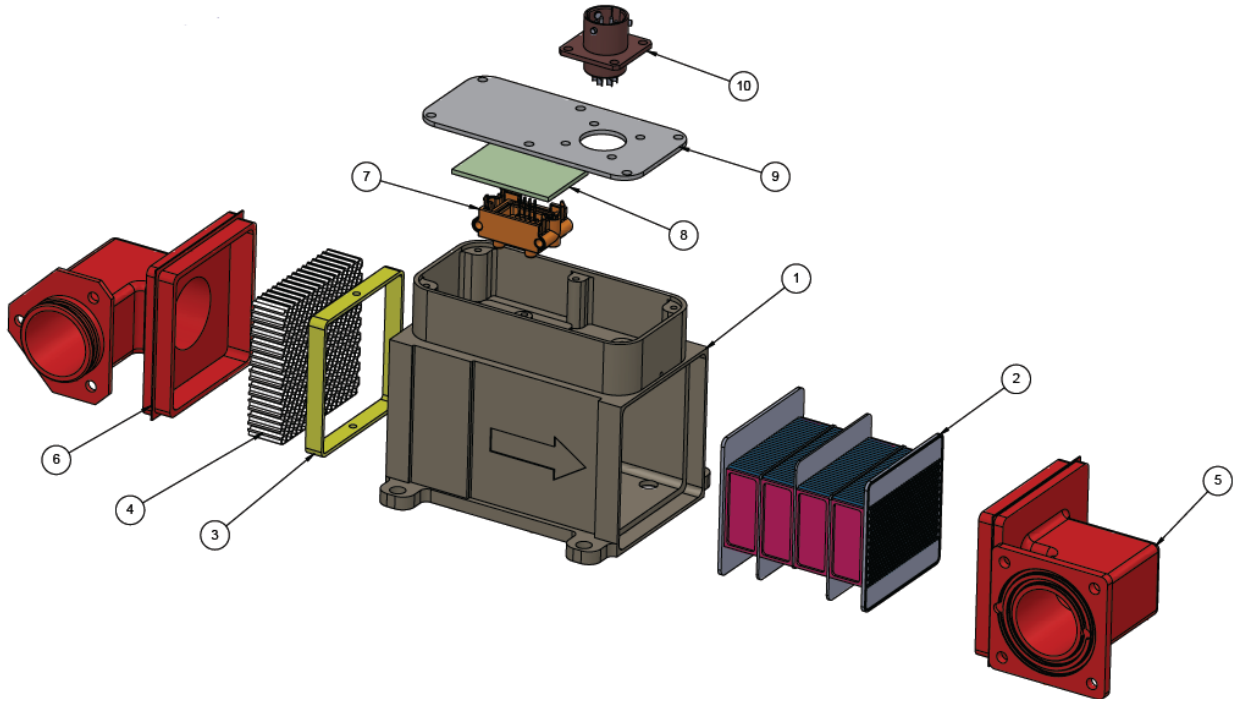

Figure 16. Assembled and exploded view of flight-like prototype FMHX.

VIII. Conclusion

This work has shown that it is feasible to produce an integrated FMHX that meets requirements for service in the exploration PLSS. We developed analytic design methods for the FMHX using both empirical design correlations and CFD methods. We used these methods to design a proof-of-concept FMHX that incorporates a prototypical FMHX core. We developed fabrication and assembly approaches and built a proof-of-concept FMHX, then measured the flow and heat transfer performance and compared with NASA requirements. The proof-of-concept unit met all requirements for pressure drop and heat transfer with significant margin. We also found that miniature, commercial, oxygen-compatible sensors were capable of generating output signals that were highly linear functions of the gas flow rate. Finally, we used the results of the proof-of-concept tests to design a flight-like FMHX that is packaged for integration with NASA PLSS test beds.

Acknowledgments

The authors gratefully acknowledge the support of NASA Lyndon B. Johnson Space Center and the NASA SBIR program.

References

[1]Idelchik, I.E., *Handbook of Hydraulic Resistance,* Second Edition Revised and Augmented, Hemisphere Publishing Corporation, 1986.

[2]Kays, W.M., and London, A.L., *Compact Heat Exchangers*, Third Editions, Krieger Publishing Company, 1984.

[3]Leinhard, J.H. V, and Leinhard, J.H. VI, *A Heat Transfer Textbook*, Fourth Edition, Dover Publications, 2011.